Supplement of

Development of an integrated model framework for multi-air-pollutant exposure assessments in high-density cities and the implications for epidemiological research

Zhiyuan Li[1,2], Kin-Fai Ho[3], Harry Fung Lee[4], Steve Hung Lam Yim[5,6,7,*]

[1]Department of Environmental Health, School of Public Health (Shenzhen), Sun Yat-sen University, Guangzhou, China
[2]Institute of Environment, Energy and Sustainability, The Chinese University of Hong Kong, Shatin, N.T., Hong Kong, China
[3]The Jockey Club School of Public Health and Primary Care, The Chinese University of Hong Kong, Shatin, N.T., Hong Kong, China
[4]Department of Geography and Resource Management, The Chinese University of Hong Kong, Shatin, N.T., Hong Kong, China
[5]Asian School of the Environment, Nanyang Technological University, Singapore
[6]Lee Kong Chian School of Medicine, Nanyang Technological University, Singapore
[7]Earth Observatory of Singapore, Nanyang Technological University, Singapore

Correspondence to: Steve Hung Lam Yim (steve.yim@ntu.edu.sg)

Table of Content

Supplement Text S1

The LUR model requires air pollutant concentration data and data inputs of the potential predictor variables (e.g., the road network and land-use types) affecting air pollutant concentration. The output of the LUR model consists of a linear regression model describing the association between the predictor variables and measured concentration, predicted concentration at the monitoring sites, and the associated measures of the model predictive accuracy (Jin et al., 2019; Lee et al., 2017; Meng et al., 2015).

The form of the LUR model can be written as follows (Cordioli et al., 2017; Liu et al., 2016; Naughton et al., 2018):

$$Y(s,t) = \beta_0(s,t) + \sum_k \beta_{1,k}(s,t)\, X_k(s,t) + \varepsilon(s,t) \qquad\qquad (Eq.\,1)$$

In the above, *Y(s,t)* is the observed air pollutant concentration at location *s* and time *t*; β_0 and $\beta_{1,k}$ are, respectively, the regression intercept and slope values, which are potentially spatially and temporally varying, but may also be constant in time and space; *X* is the independent variable (e.g., population density and urban/building morphology data); *k* is the predictor variable type; and $\varepsilon(s,t)$ is the residual error term at location *s* and time *t*, representing the unexplained variation in concentration.

Supplement Text S2

The R^2 value of these LUR models varies a lot between cities, from around 0.20 to above 0.90 (Cai et al., 2020; Li et al., 2021;

30   Hoek et al., 2008; Xu et al., 2019). The performance of recent PM$_{2.5}$ LUR studies included R^2 values of 0.65 for Shanghai, China (Cai et al., 2020), 0.47 for Southern California, USA (Jones et al., 2020), 0.86 for Beijing, China (Xu et al., 2019), 0.75 for Nanjing, China (Huang et al., 2017), 0.77 for Lanzhou, China (Jin et al., 2019), 0.59 for Hong Kong, China (Lee et al., 2017), and 0.71 for Sabzevar, Iran (Miri et al., 2019). For NO$_2$ LUR models, the R^2 values were 0.73 for Shanghai, China (Cai et al., 2020), 0.82 for Shanghai, China (Meng et al., 2015), 0.87 for Nanjing, China (Huang et al., 2017), 0.71 for Lanzhou, China (Jin et al., 2019), 0.46

35   for Hong Kong, China (Lee et al., 2017), 0.66 for Auckland, New Zealand (Ma et al., 2019), and 0.84 for Sydney, Australia (Cowie et al., 2019). Compared with PM$_{2.5}$ and NO$_2$, the number of studies for PM$_{10}$ and O$_3$ LUR models is relatively limited. PM$_{10}$ LUR models have been established with R^2 values of 0.80 in Shanghai, China (Meng et al., 2016), 0.75 in Sabzevar, Iran (Miri et al., 2019), and 0.38 in Mexico City, Mexico (Son et al., 2018), and 0.95 for Manchester, UK (Mölter and Lindley, 2021). The R^2 values for O$_3$ LUR models were 0.92 for Augsburg, Germany (Wolf et al., 2017), 0.72–0.98 for Tianjin, China (Wang et al., 2020), and

40   0.65 for Nanjing, China (Huang et al., 2017). The spatial resolution of the air pollution surface depends on the spatial resolution of the input data, and is typically in hundreds of meters of resolution (Cai et al., 2020; Li et al., 2021; Meng et al., 2015; Xu et al., 2019). Recent studies have successfully downscaled the spatial-resolution to finer scales, of tens of meters (Li et al., 2018; Luminati et al., 2021; Ma et al., 2019; Naughton et al., 2018; Son et al., 2018).

Table S1. A description of the air quality monitoring stations in Hong Kong.

Station	Location	Station type	Sampling height (above the sea level)	Date start operation
Central/Western	2 High Street, Sai Ying Pun	Urban: Mixed residential/commercial	82 m	Nov 1983
Eastern	20 Wai Hang Street, Sai Wan Ho	Urban: Residential	28 m	Jan 1999
Kwun Tong	407-431 Kwun Tong Road, Kwun Tong	Urban: Mixed residential/commercial/industrial	37 m	Jul 1983
Sham Shui Po	37A Yen Chow Street, Sham Shui Po	Urban: Mixed residential/commercial	21 m	Jul 1984
Kwai Chung	999 Kwai Chung Road, Kwai Chung	Urban: Mixed residential/commercial/industrial	19 m	Jul 1988
Tsuen Wan	60 Tai Ho Road, Tsuen Wan	Urban: Mixed residential/commercial/industrial	21 m	Aug 1988
Tseung Kwan O	9 Wan Lung Road, Tseung Kwan O, Sai Kung	Urban: Residential	23 m	Mar 2016
Yuen Long	269 Castle Peak Road, Yuen Long	New Town: Residential	31 m	Jul 1995
Tuen Mun	1 Tuen Hi Road, Tuen Mun	New Town: Residential	31 m	Dec 2013
Tung Chung	6 Fu Tung Street, Tung Chung	New Town: Residential	34.5 m	Apr 1999
Tai Po	1 Ting Kok Road, Tai Po	New Town: Residential	31 m	Feb 1990
Sha Tin	11-17 Man Lai Road, Tai Wai, Sha Tin	New Town: Residential	31 m	Jul 1991
Tap Mun	Tap Mun Police Post	Background: Rural	26 m	Apr 1998
Causeway Bay	1 Yee Woo Street, Causeway Bay	Urban Roadside: Mixed commercial/residential area surrounded by tall buildings	6.5 m [a] / 7 m [b]	Jan 1998
Central	Junction of Des Voeux Road Central and Chater Road, Central	Urban Roadside: Busy commercial/financial area surrounded by tall buildings	8.5 m	Oct 1998
Mong Kok	Junction of Nathan Road and Lai Chi Kok Road, Mong Kok	Urban Roadside: Mixed commercial/residential area surrounded by tall buildings	8.5 m [a] / 10.9 m [b]	Apr 1991

45

Note: [a] Sampling height for gaseous pollutants.

[b] Sampling height for suspended particulates.

Table S2. Meteorological data and the geo-spatial data used for the LUR modelling.

Category	Variables	Buffer size (radius in meters)	Data sources
Air quality data	PM_{10}, $PM_{2.5}$, NO_2, O_3, etc.	NA	Hong Kong Environmental Protection Department
Land use data	Residential area, farmland, green space, water body, etc.	50 m, 100 m, 300 m, 500 m, 700 m, 1000 m, 2000 m, 3000 m, 4000m, and 5000 m	Hong Kong Planning Department
Meteorological data	Temperature, relative humidity, wind speed, wind direction, etc.	NA	Hong Kong Observatory
Road network	Road length, private light bus, bus, car, taxi, van, light duty vehicle, medium duty vehicle, heavy duty vehicle, truck, canyon height	50 m, 100 m, 300 m, 500 m, 700 m, 1000 m, 2000 m, 3000 m, 4000m, and 5000 m	Hong Kong Transportation Department
Population data	Population count	50 m, 100 m, 300 m, 500 m, 700 m, 1000 m, 2000 m, 3000 m, 4000m, and 5000 m	Hong Kong Census and Statistics Department
Topography data	Elevation	NA	Chinese Academy of Sciences
Urban/building morphology	Building height, building area	50 m, 100 m, 300 m, 500 m, 700 m, 1000 m, 2000 m, 3000 m, 4000m, and 5000 m	Hong Kong Planning Department
Geo-location	Longitude, Latitude	NA	Hong Kong Environmental Protection Department

50

Table S3. Description of the annual-average LUR models for ambient PM_{10}, PM_{10} TC, PM_{10} NO_3^-, PM_{10} SO_4^{2-}, PM_{10} Cd, $PM_{2.5}$, NO_2, and O_3 in Hong Kong.

Air pollutant	Variable	Coefficient	Standard error	P	VIF	Predictive accuracy
PM_{10}	Constant	24.6	1.46	<0.001	NA	$R^2 = 0.92$; LOOCV R^2 = 0.77.
	F_CARVL100	1.54×10^{-3}	2.32×10^{-4}	<0.001	1.1	
	Area_S_100	1.15×10^{-3}	1.53×10^{-4}	<0.001	1.6	
	Res_100	8.47×10^{-4}	1.26×10^{-4}	<0.001	1.4	
	Ind_3000	1.73×10^{-6}	4.24×10^{-7}	0.003	1.4	
	Ins_4000	-1.44×10^{-6}	3.82×10^{-7}	0.004	1.7	
PM_{10} TC	Constant	4808	199.4	<0.001	NA	$R^2 = 0.94$; LOOCV R^2 = 0.73.
	F_Bus50	4.79×10^{-1}	6.40×10^{-2}	<0.001	1.1	
	F_MHGVVL700	6.67×10^{-2}	1.21×10^{-2}	0.001	1.1	
PM_{10} NO_3^-	Constant	2282	169.0	<0.001	NA	$R^2 = 0.93$; LOOCV R^2 = 0.88.
	F_CARVL500	4.10×10^{-2}	6.76×10^{-3}	0.001	1.3	
	Area_S_300	9.88×10^{-3}	2.60×10^{-3}	0.007	1.3	
PM_{10} SO_4^{2-}	Constant	6295	95.0	<0.001	NA	$R^2 = 0.97$; LOOCV R^2 = 0.92.
	F_TVL100	3.66×10^{-2}	2.95×10^{-3}	<0.001	1.2	
	H_M_700	1.49	2.72×10^{-1}	0.002	1.1	
	Tra_1000	2.76×10^{-4}	1.04×10^{-4}	0.037	1.1	
PM_{10} Cd	Constant	-19.3	3.73	0.002	NA	$R^2 = 0.92$; LOOCV R^2 = 0.76.
	Tra_2000	4.24×10^{-8}	7.28×10^{-9}	0.001	1.0	
	Lat	8.85×10^{-1}	1.66×10^{-1}	0.002	2.3	
	RH_A300	3.82×10^{-3}	1.23×10^{-3}	0.021	2.3	
$PM_{2.5}$	Constant	15.6	1.74	<0.001	NA	$R^2 = 0.91$; LOOCV R^2 = 0.81.
	F_LGVVL500	7.55×10^{-4}	9.03×10^{-5}	<0.001	3.8	
	Ins_4000	-2.68×10^{-6}	4.71×10^{-7}	<0.001	4.0	
	Res_300	5.78×10^{-5}	1.13×10^{-5}	0.001	1.3	
	Area_S_50	1.92×10^{-3}	4.72×10^{-4}	0.003	1.2	
	H_M_100	1.67×10^{-2}	6.82×10^{-3}	0.040	1.2	
NO_2	Constant	9.27	4.61	0.07	NA	$R^2 = 0.96$; LOOCV R^2 = 0.93.
	F_TVL500	3.73×10^{-4}	2.79×10^{-5}	< 0.001	1.7	
	POP_100	6.62×10^{-4}	1.54×10^{-4}	0.001	1.6	
	Ind_1000	3.12×10^{-5}	1.17×10^{-5}	0.022	1.1	
O_3	Constant	-5944	1557	0.003	NA	$R^2 = 0.92$; LOOCV R^2 = 0.87.
	F_TVL700	-1.20×10^{-4}	1.55×10^{-5}	< 0.001	1.4	
	Lon	52.5	13.6	0.003	1.1	
	Ins_300	1.18×10^{-4}	5.35×10^{-5}	0.049	1.4	

- F_CARVL100, F_CARVL500: the number of private cars within 100-m and 500-m buffers
- Area_S_50, Area_S_100, Area_S_300: the area of buildings within 50-m, 100-m, and 300-m buffers
- Res_100, Res_300: the area of residential land within 100-m and 300-m buffers
- Ind_1000, Ind_3000: the area of industrial land within 1000-m and 3000-m buffers
- Ins_300, Ins_4000: the area of urban green space within 300-m and 4000-m buffers
- F_BUS50: the number of buses within a 50-m buffer
- F_MHGVVL700: the number of medium & heavy-duty vehicles within a 700-m buffer
- F_TVL100, F_TVL500, F_TVL700: the number of total vehicles within 100-m, 500-m, and 700-m buffers

- H_M_100, H_M_700: the maximum building height within 100-m and 700-m buffers
- Tra_1000, Tra_2000: the area of transportation land within 1000-m and 2000-m buffers
- RH_A300: the average canyon height within a 300-m buffer

65
- F_LGVVL500: the number of light-duty vehicles within a 500-m buffer
- POP_100: the number of people within a 100-m buffer
- Lat and Lon: latitude and longitude
- VIF: the Variance Inflation Factor
- LOOCV: leave-one-out cross-validation

70
- NA: not applicable

Table S4. Statistical description of concentration estimates of ambient PM_{10}, $PM_{2.5}$, NO_2, O_3 ($\mu g/m^3$), and PM_{10} TC, PM_{10} NO_3^-, PM_{10} SO_4^{2-}, PM_{10} Cd (ng/m^3) for the grid cells using LUR models.

Air pollutants	Mean	Standard deviation	Minimum	Maximum
PM_{10}	27.1	7.87	15.3	55.0
PM_{10} TC	5207	997	4808	13555
PM_{10} NO_3^-	2607	655	2282	6867
PM_{10} SO_4^{2-}	6552	264	6295	8791
PM_{10} Cd	0.53	0.10	0.28	0.90
$PM_{2.5}$	15.4	6.77	0.00	47.1
NO_2	17.7	16.3	9.27	117.3
O_3	49.3	11.3	0.29	89.8

75   **Table S5.** The average LUR estimated ambient PM_{10}, $PM_{2.5}$, NO_2, O_3 (µg/m³), and PM_{10} TC, PM_{10} NO_3^-, PM_{10} SO_4^{2-}, PM_{10} Cd (ng/m³) in the eighteen districts of Hong Kong.

District	PM_{10}	PM_{10} TC	PM_{10} NO_3^-	PM_{10} SO_4^{2-}	PM_{10} Cd	$PM_{2.5}$	NO_2	O_3
Wong Tai Sin	32.04	6134	3491	6988	0.59	19.65	40.70	39.60
Kowloon City	31.23	6283	4065	6845	0.62	19.26	49.88	33.20
Kwun Tong	35.26	5968	3750	6877	0.62	24.93	52.48	39.57
Sai Kung	24.84	4862	2409	6472	0.49	13.19	12.04	61.64
North	27.49	5007	2455	6453	0.62	14.73	14.58	54.37
Central & Western	29.87	5072	3367	7133	0.53	16.52	31.50	41.80
Wan Chai	27.12	5123	3419	6926	0.51	14.57	31.50	42.70
Eastern	28.23	5029	2819	6823	0.49	14.94	21.35	53.77
Tuen Mun	27.12	5472	2563	6510	0.53	15.12	16.88	41.52
Yuen Long	32.24	5318	2651	6506	0.58	17.10	22.97	45.31
Southern	25.00	4846	2535	6610	0.40	12.64	14.15	55.70
Islands	24.70	4840	2356	6490	0.38	14.63	10.10	43.28
Sham Shui Po	36.97	8198	4588	6981	0.66	29.33	64.98	22.80
Yau Tsim Mong	36.48	7759	5101	7198	0.68	31.56	79.78	14.35
Kwai Tsing	30.56	7768	3314	6877	0.64	20.96	43.18	34.83
Tsuen Wan	25.73	5451	2586	6722	0.52	15.77	17.63	45.81
Tai Po	25.68	5023	2456	6473	0.56	14.72	12.87	56.28
Sha Tin	24.79	5349	2779	6710	0.55	13.20	18.85	50.94

80 **Figure S1.** The location of sixteen air quality monitoring stations (AQMSs) in Hong Kong, of which thirteen are general AQMSs including Yuen Long (YL), Tung Chung (TC), Tsuen Wan (TW), Kwai Chung (KC), Sham Shui Po (SSP), Sha Tin (ST), Tai Po (TP), Tap Mun (TM), Tuen Mun (TUM), Tseung Kwan O (TKO), Kwun Tong (KT), Eastern (EN), Central/Western (CW), and three are roadside AQMSs including Mong Kok (MK), Central (CN), and Causeway Bay (CB).
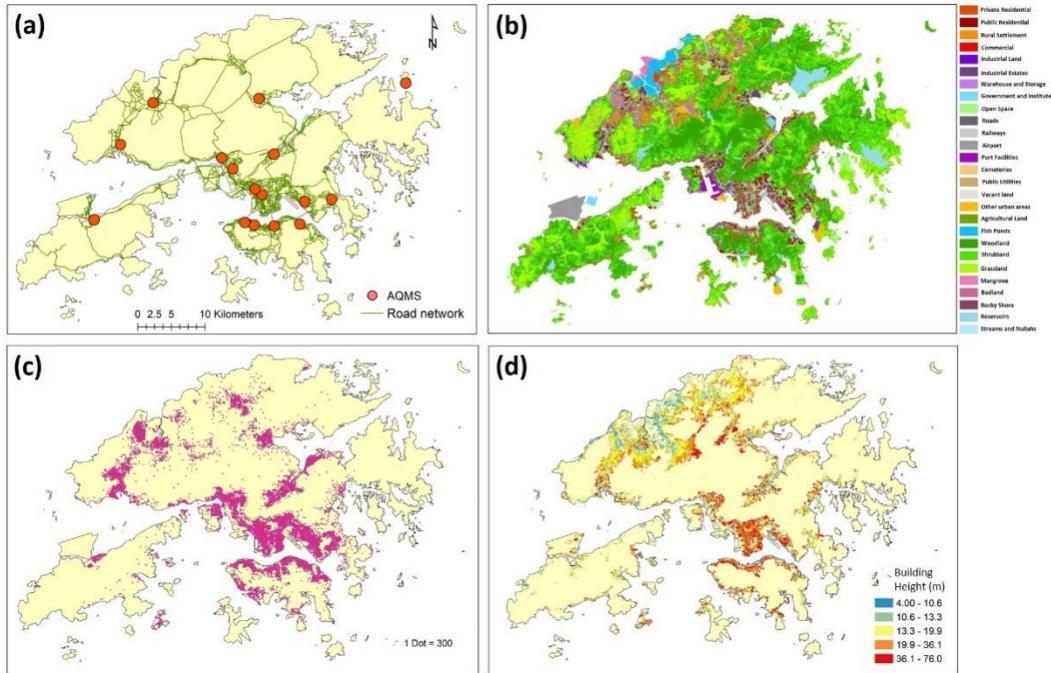
85

Figure S2. The geospatial data within the study area. (a) The road network with the 16 air quality monitoring stations. (b) Land-use types. (c) Population density. (d) Building morphology.
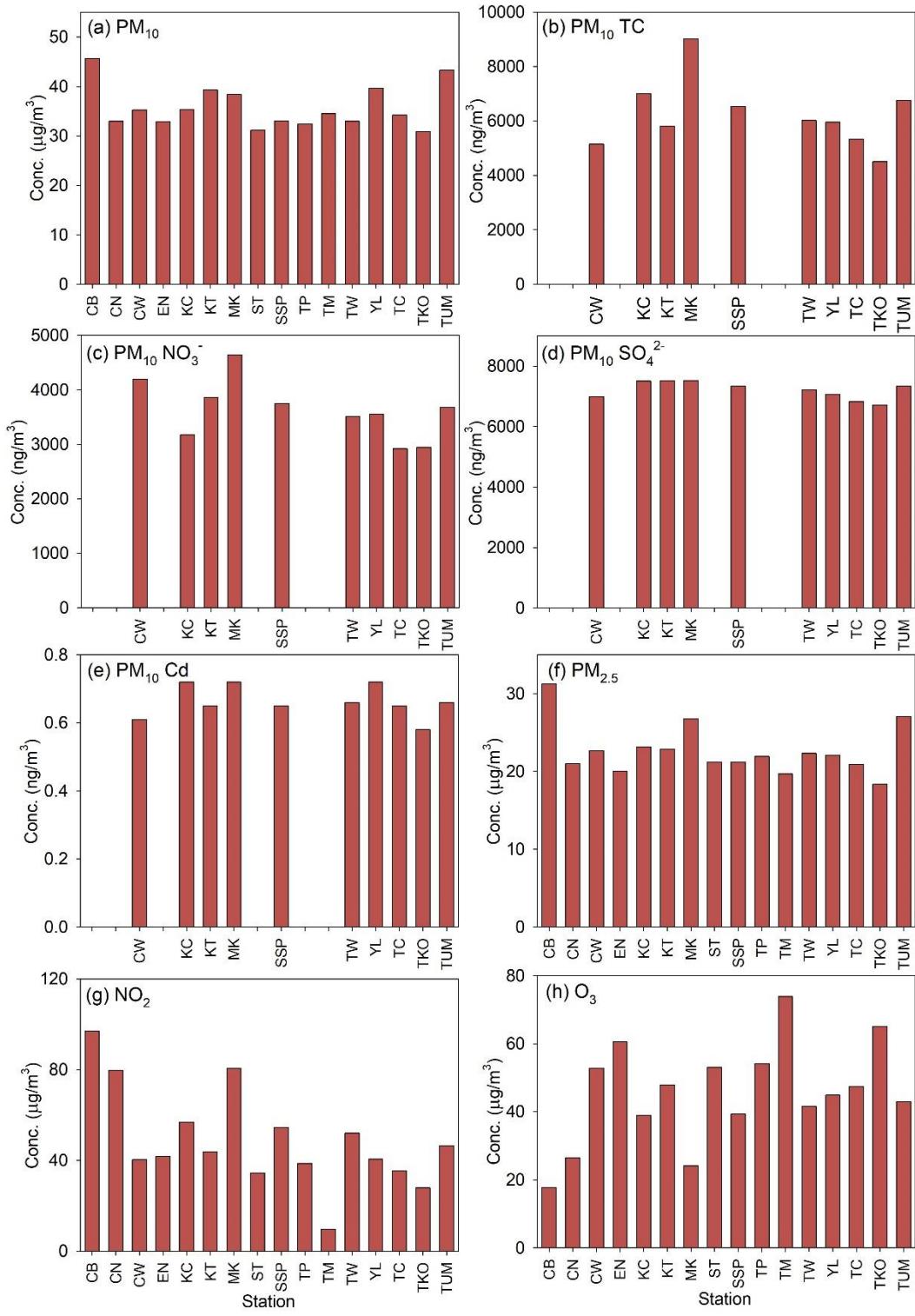
90 **Figure S3.** Annual-average concentration of PM$_{10}$, PM$_{2.5}$, NO$_2$, O$_3$, and four major PM$_{10}$ chemical species at general and roadside stations.
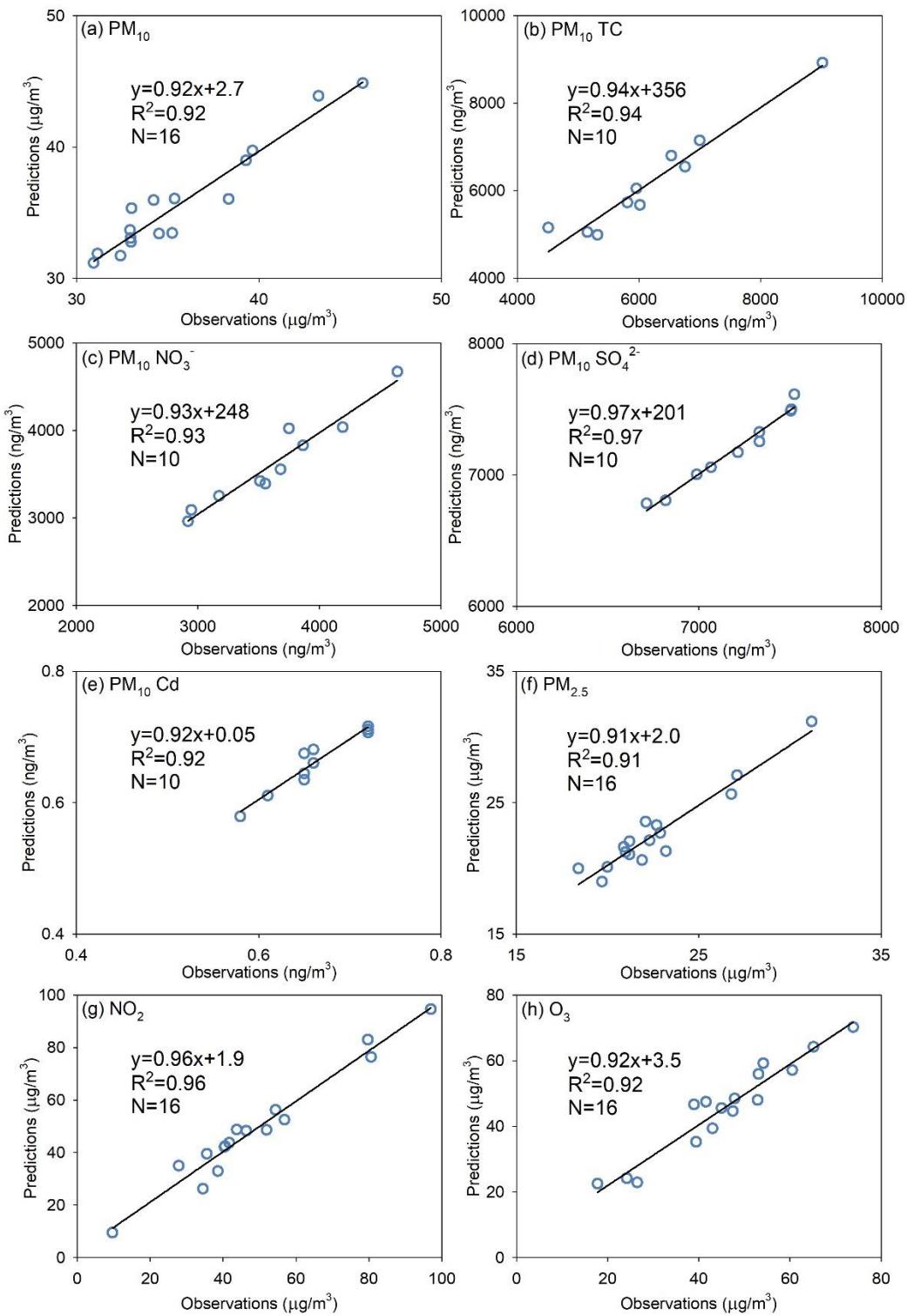
Figure S4. A comparison of LUR-predicted concentration and observed concentration of the studied air pollutants.
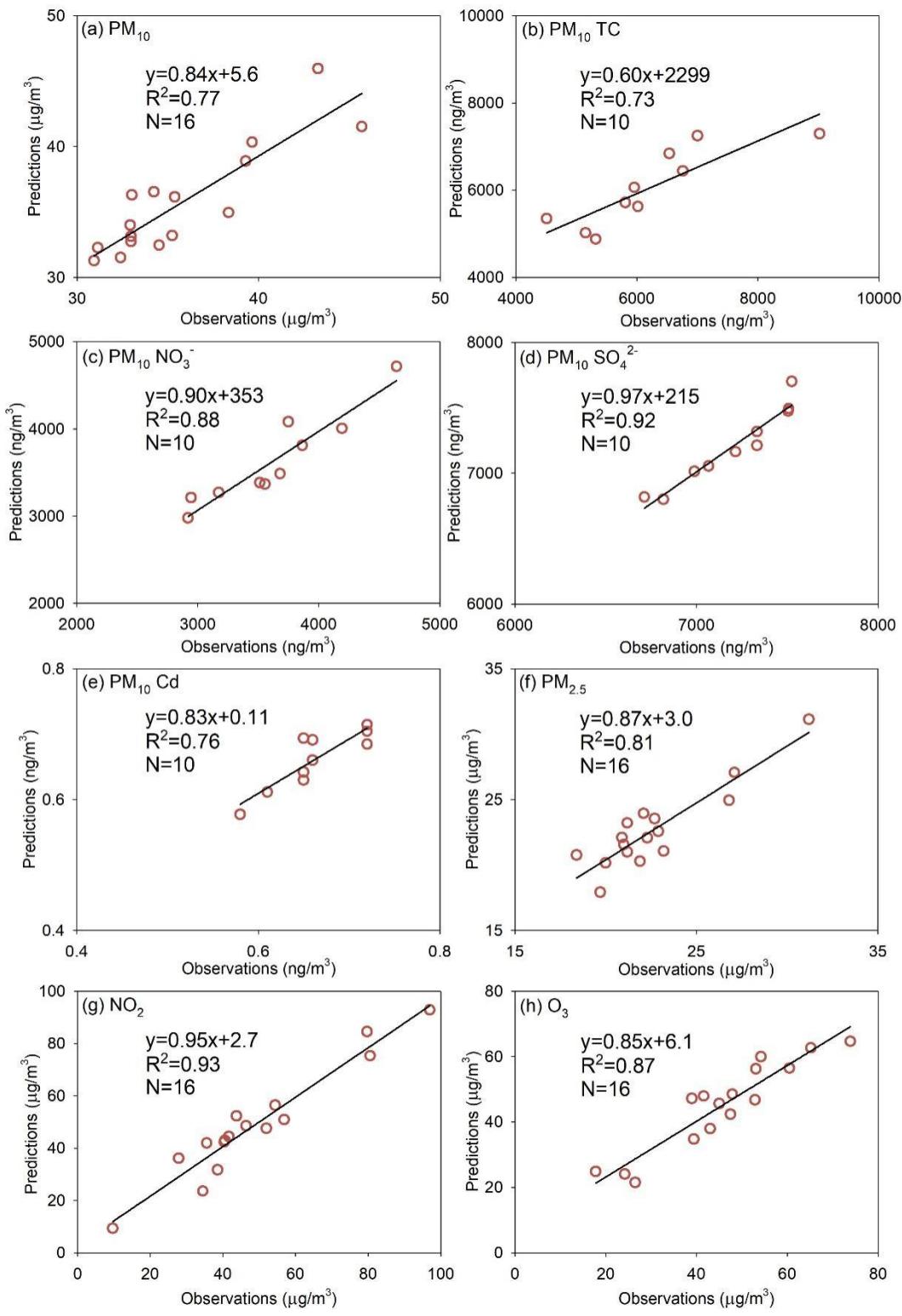
Figure S5. A comparison of LOOCV-predicted concentration and observed concentration of the studied air pollutants.
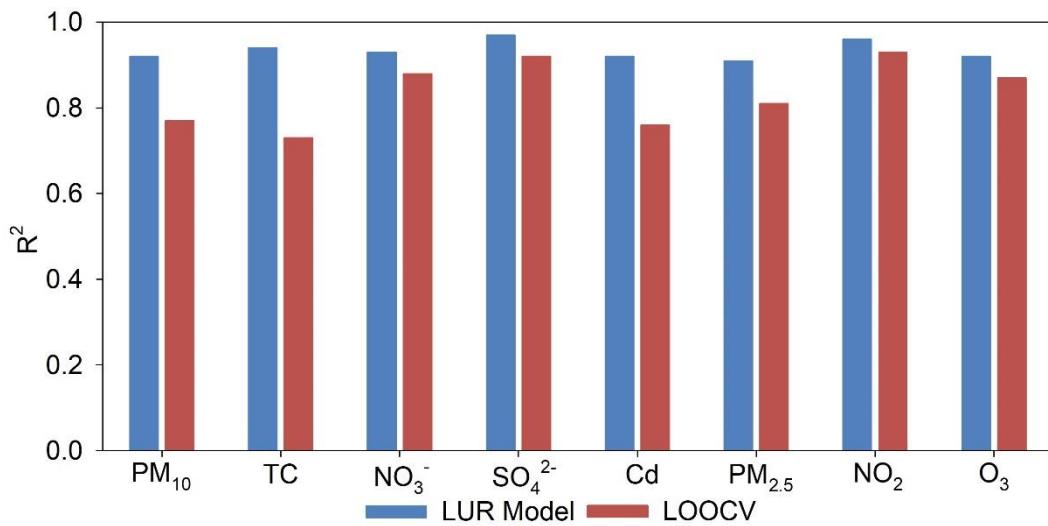
Figure S6. The model and leave-one-out cross-validation (LOOCV) R^2 values for PM_{10}, PM_{10} TC, PM_{10} NO_3^-, PM_{10} SO_4^{2-}, PM_{10} Cd, $PM_{2.5}$, NO_2, and O_3. All the established models were statistically significant.

100

(a)

Air pollutants	Moran's Index	z-score	p-value	Interpretation
PM_{10}	-0.048	0.399	0.689	
PM_{10} TC	-0.163	-0.249	0.804	
PM_{10} NO_3^-	-0.012	0.453	0.650	Do not appear to
PM_{10} SO_4^{2-}	-0.184	-0.504	0.615	be significantly
PM_{10} Cd	-0.292	-0.843	0.399	different than
$PM_{2.5}$	-0.122	-0.571	0.568	random.
NO_2	0.025	0.935	0.350	
O_3	0.051	1.186	0.236	
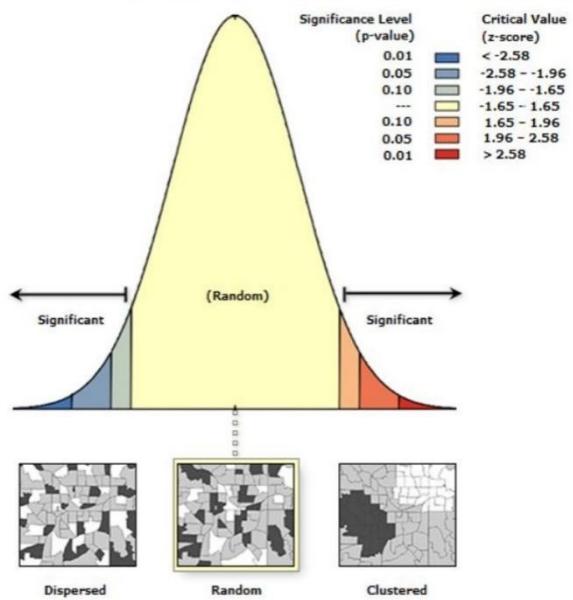
Figure S7. Moran's *I* index values of concentration residuals for the LUR models. (a) The spatial autocorrelation analysis results using the ArcGIS software. (b) The definition of Moran's *I* analysis results.

105
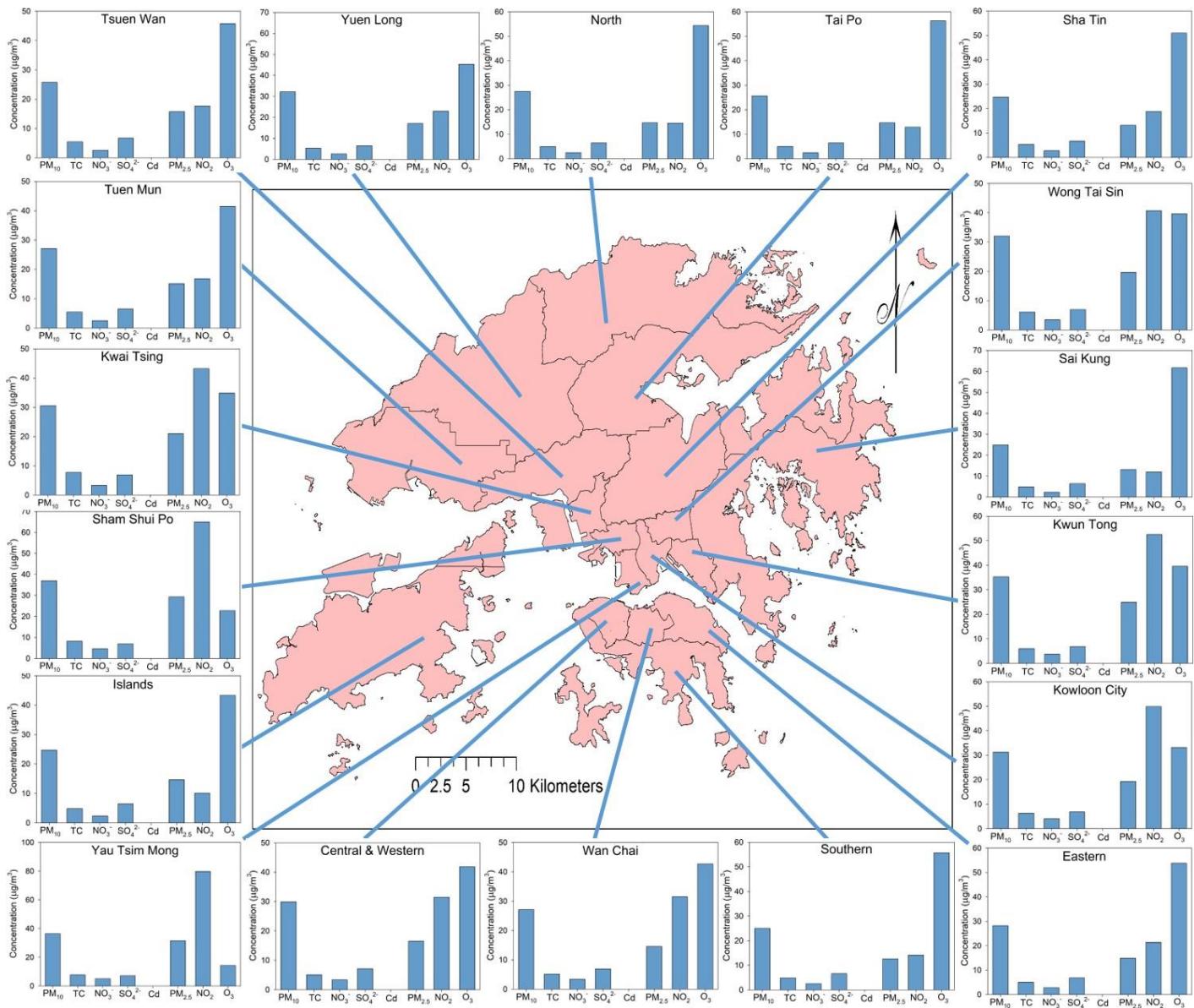
Figure S8. The distribution of the average LUR estimated ambient PM_{10}, $PM_{2.5}$, NO_2, O_3 ($\mu g/m^3$), and PM_{10} TC, PM_{10} NO_3^-, PM_{10} SO_4^{2-}, PM_{10} Cd (ng/m^3) in the eighteen districts of Hong Kong.

References

Cai, J., Ge, Y., Li, H., Yang, C., Liu, C., Meng, X., Wang, W., Niu, C., Kan, L., Schikowski, T., and Yan, B.: Application of land use regression to assess exposure and identify potential sources in PM$_{2.5}$, BC, NO$_2$ concentrations. Atmos. Environ. 223, 117267, 2020.

Cordioli, M., Pironi, C., De Munari, E., Marmiroli, N., Lauriola, P., and Ranzi, A.: Combining land use regression models and fixed site monitoring to reconstruct spatiotemporal variability of NO$_2$ concentrations over a wide geographical area. Sci. Total Environ. 574, 1075-1084, 2017.

Cowie, C.T., Garden, F., Jegasothy, E., Knibbs, L.D., Hanigan, I., Morley, D., Hansell, A., Hoek, G., and Marks, G.B.: Comparison of model estimates from an intra-city land use regression model with a national satellite-LUR and a regional Bayesian Maximum Entropy model, in estimating NO$_2$ for a birth cohort in Sydney, Australia. Environ. Res. 174, 24-34, 2019.

Hoek, G., Beelen, R., De Hoogh, K., Vienneau, D., Gulliver, J., Fischer, P., and Briggs, D.: A review of land-use regression models to assess spatial variation of outdoor air pollution. Atmos. Environ. 42(33), 7561-7578, 2008.

Huang, L., Zhang, C., and Bi, J.: Development of land use regression models for PM$_{2.5}$, SO$_2$, NO$_2$ and O$_3$ in Nanjing, China. Environ. Res. 158, 542-552, 2017.

Jin, L., Berman, J.D., Warren, J.L., Levy, J.I., Thurston, G., Zhang, Y., Xu, X., Wang, S., Zhang, Y., and Bell, M.L.: A land use regression model of nitrogen dioxide and fine particulate matter in a complex urban core in Lanzhou, China. Environ. Res. 177, 108597, 2019.

Jones, R.R., Hoek, G., Fisher, J.A., Hasheminassab, S., Wang, D., Ward, M.H., Sioutas, C., Vermeulen, R., and Silverman, D.T.: Land use regression models for ultrafine particles, fine particles, and black carbon in southern California. Sci. Total Environ. 699, 134234, 2020.

Lee, M., Brauer, M., Wong, P., Tang, R., Tsui, T.H., Choi, C., Cheng, W., Lai, P.C., Tian, L., Thach, T.Q., and Allen, R.: Land use regression modelling of air pollution in high density high rise cities: A case study in Hong Kong. Sci Total Environ. 592, 306-315, 2017.

Li, R., Ma, T., Xu, Q., and Song, X.: Using MAIAC AOD to verify the PM$_{2.5}$ spatial patterns of a land use regression model. Environ. Pollut. 243, 501-509, 2018.

Li, Z., Ho, K.F., Chuang, H.C., and Yim, S.H.L.: Development and intercity transferability of land-use regression models for predicting ambient PM$_{10}$, PM$_{2.5}$, NO$_2$ and O$_3$ concentrations in northern Taiwan. Atmos. Chem. Phys. 21, 5063–5078, 2021.

Liu, C., Henderson, B.H., Wang, D., Yang, X., and Peng, Z.R.: A land use regression application into assessing spatial variation of intra-urban fine particulate matter (PM$_{2.5}$) and nitrogen dioxide (NO$_2$) concentrations in City of Shanghai, China. Sci. Total Environ. 565, 607-615, 2016.

Luminati, O., de Campos, B.L.D.A., Flückiger, B., Brentani, A., Röösli, M., Fink, G., and de Hoogh, K.: Land use regression modelling of NO$_2$ in Sao Paulo, Brazil. Environ. Pollut. 289, 117832, 2021.

Ma, X., Longley, I., Gao, J., Kachhara, A., and Salmond, J.: A site-optimised multi-scale GIS based land use regression model for simulating local scale patterns in air pollution. Sci. Total Environ. 685, 134-149, 2019.

Meng, X., Chen, L., Cai, J., Zou, B., Wu, C.F., Fu, Q., Zhang, Y., Liu, Y., and Kan, H.: A land use regression model for estimating the NO$_2$ concentration in Shanghai, China. Environ. Res. 137, 308-315, 2015.

Meng, X., Fu, Q., Ma, Z., Chen, L., Zou, B., Zhang, Y., Xue, W., Wang, J., Wang, D., Kan, H., and Liu, Y.: Estimating ground-level PM$_{10}$ in a Chinese city by combining satellite data, meteorological information and a land use regression model. Environ. Pollut. 208, 177-184, 2016.

Miri, M., Ghassoun, Y., Dovlatabadi, A., Ebrahimnejad, A., and Löwner, M.O.: Estimate annual and seasonal PM$_1$, PM$_{2.5}$ and PM$_{10}$ concentrations using land use regression model. Ecotoxicol. Environ. Saf. 174, 137-145, 2019.

Mölter, A., and Lindley, S.: Developing land use regression models for environmental science research using the XLUR tool– More than a one-trick pony. Environ. Model. Softw. 143, 105108, 2021.

Naughton, O., Donnelly, A., Nolan, P., Pilla, F., Misstear, B.D., and Broderick, B.: A land use regression model for explaining spatial variation in air pollution levels using a wind sector based approach. Sci. Total Environ. 630, 1324-1334, 2018.

Son, Y., Osornio-Vargas, Á.R., O'Neill, M.S., Hystad, P., Texcalac-Sangrador, J.L., Ohman-Strickland, P., Meng, Q., and Schwander, S.: Land use regression models to assess air pollution exposure in Mexico City using finer spatial and temporal input parameters. Sci. Total Environ. 639, 40-48, 2018.

Wang, J., Cohan, D.S., and Xu, H.: Spatiotemporal ozone pollution LUR models: Suitable statistical algorithms and time scales for a megacity scale. Atmos. Environ. 237, 117671, 2020.

Wolf, K., Cyrys, J., Harciníková, T., Gu, J., Kusch, T., Hampel, R., Schneider, A., and Peters, A.: Land use regression modeling of ultrafine particles, ozone, nitrogen oxides and markers of particulate matter pollution in Augsburg, Germany. Sci. Total Environ. 579, 1531-1540, 2017.

Xu, M., Sbihi, H., Pan, X., and Brauer, M.: Local variation of $PM_{2.5}$ and NO_2 concentrations within metropolitan Beijing. Atmos. Environ. 200, 254-263, 2019.

160